Published in final edited form as:
Inorg Chem. 2009 February 2; 48(3): 971–977. doi:10.1021/ic801617q.

Tetragonal to Triclinic — A Phase Change for [Fe(TPP)(NO)]

Nathan J. Silvernail[†], **Marilyn M. Olmstead**[‡,*], **Bruce C. Noll**[†], and **W. Robert Scheidt**[*,†]

†*Department of Chemistry and Biochemistry, University of Notre Dame, Notre Dame, Indiana 46556*

‡*Department of Chemistry, Davis, California 95616*

Abstract

The temperature-dependence of the crystalline phase of (nitrosyl)(tetraphenylpor-phinato)iron(II), [Fe(TPP)(NO)], has been explored over the temperature range of 33 to 293 K. The crystalline complex is found in the tetragonal crystal system at higher temperatures and in the triclinic crystal system at lower temperatures. In the tetragonal system, the axial ligand is strongly disordered with the molecule having crystallographically required 4/*m* symmetry leading to eight distinct positions of the single nitrosyl oxygen atom. The phase transition to the triclinic crystal system leads to a partial ordering with the molecule now having inversion symmetry and disorder of the axial nitrosyl ligand over only two positions. The increase in ordering allows subtle molecular geometry features to be observed, in particular an off-axis tilt of the Fe–N_{NO} bond from the heme normal is apparent. The transition of the reversible phase change begins at about 250 K. This transition has been confirmed by both X-ray diffraction studies and a differential scanning calorimetry study.

Introduction

The perception and understanding of nitric oxide has changed from that of merely a toxic gas to that of an essential cellular signaling agent.[1] NO coordination to heme proteins has many physiological consequences. It has been implicated in a number of fundamental processes including smooth muscle relaxation,[2, 3] platelet deaggregation,[4] neuronal communication,[5] aspects of myocardial function, and numerous other physiological functions.[6] NO is synthesized by nitric oxide synthase through a heme-mediated oxidation of L-arginine[7, 8, 9] or from NO_3^-/NO_2^-.[10] In many of these biochemical processes, the binding of NO to a heme protein and the labilization or loss of the ligand trans to the NO or another rearrangement is the significant signalling event resulting in a five-coordinate heme-NO active complex.

Five-coordinate [Fe(TPP)(NO)][11] was originally characterized in this laboratory in 1975.[12] Although this was more than a decade before the known biological importance of NO, this investigation provided the first insight into the coordination chemistry of NO to heme. Some of the structural features were obscured as a result of the 4/*m* symmetry of the molecular center in the *I*4/*m* crystal system. The molecule had an eight-fold disorder of the NO oxygen, an Fe–N_{NO} bond exactly perpendicular to the porphyrin plane, and phenyl rings rotated exactly 90° from the porphyrin plane. Subsequent structural investigations of well-resolved heme-NO complexes utilizing octaethylporphyrin more precisely detailed the geometrical parameters of the heme-NO complex.[13, 14] Some of the more salient observations were the off-axis tilting of the Fe–N_{NO} vector from the heme normal. An equatorial asymmetry observed in the Fe–N_p distances with a short pair of bonds bracketing the projection of the tilted and bent NO ligand onto the porphyrin core. These observations were further noted and the electronic basis

*To whom correspondence should be addressed: E-mail E-mail: mmolmstead@ucdavis.edu, E-mail: scheidt.1@nd.edu.

for the tilt and the equatorial asymmetry was subsequently recognized in several DFT calculations.[15, 16, 17, 18].

In solid-state vibrational studies utilizing the NRVS technique,[19] a substantial temperature-dependent variation in the Fe–N_{NO} stretch was noted.[20] A low-temperature crystallographic study of [Fe(TPP)(NO)] showed that there was an apparent phase change. This led to the substantial temperature-dependent study of the phase change and the resulting phenomenon that accompanies the phase change. The resulting order-disorder phase change, which is completely reversible, is reported herein. The phase change also leads to the observation that, at low temperatures, the structure of [Fe(TPP)(NO)] shows the off-axis tilting of the Fe–N_{NO} bond seen in a number of other iron nitrosyl species.

Experimental Section

General Information

All reactions were carried out under anaerobic conditions using standard Schlenk techniques under an argon atmosphere. All solvents were freeze/pump/thaw degassed (×3) prior to use. Methanol (Acros) and pyridine (Fisher) were used as received. Nitric oxide (Mittler Specialty Gases) was purified by passing it through a trap containing 4 Å molecular sieves immersed in an ethanol/dry ice slurry.[21] Free base porphyrin [H_2TPP] was prepared according to Adler et al.[22] [Fe(TPP)(Cl)] was prepared according to the metalation procedure of Adler et al.[23] IR measurements were taken on a Nicolet Nexus 670 FT-IR spectrometer. Selected single crystals were ground/mixed minimally with KBr. An approximately 50:1 (KBr:[Fe(TPP)(NO)]) mixture was formed into a pellet using a hydraulic press.

Synthesis of [Fe(TPP)(NO)]

[Fe(TPP)(NO)] was prepared using a modification of the previously reported synthesis.[12] A solution of 100 mg of [Fe(TPP)(Cl)], 3 mL of chloroform, 0.2 mL of methanol and 0.05 mL of pyridine was placed in a Schlenk flask and freeze/pump/thaw degassed (×3). The solution was then purged with argon for 5 min followed by bubbling of NO for approximately 5 min. Upon addition of NO the solution turns from brown to brown-orange and the final solution may contain some undissolved material. [Fe(TPP)(NO)] was then precipitated by addition of 100 mL of methanol with thorough stirring. The [Fe(TPP)(NO)] precipitate was isolated by filtration onto sintered glass. Crystals of [Fe(TPP)(NO)] were prepared by dissolving twenty-five milligrams (0.04 mmol) of the isolated solid in 7 mL of chloroform and carefully layering the solution in 8 mm glass tubes with degassed methanol followed by flame sealing. X-ray quality crystals of [Fe(TPP)(NO)] were isolated after 10 d at room temperature. IR ν_{NO} in KBr: 1700 cm^{-1}. *Note*: if KBr is not thoroughly dried, to > 130 °C, an additional ν_{NO} band is present at 1677 cm^{-1}. This band is irreversibly converted on heating of the KBr pellet (to the 1700 peak).

X-Ray Crystallographic Studies

Four distinct single crystals were indexed at 8 temperatures in ascending and descending order using a Bruker D8 Apex II system, with graphite-monochromated Mo Kα (λ = 0.71073 Å) radiation from 33–293 K (CRYO Industries or 700 Series Oxford Cryostream).[24] Crystals at 273, 290 and 293 K could be indexed as tetragonal (I-centered), whereas crystals at 33, 90, 100, 130 and 180 K could be indexed in the triclinic crystal system in the space group $P\bar{1}$. Cell parameters and crystal domains were further investigated using cell now.[26] All examples of the triclinic phase are composed of four domains related by ~90 or ~180° rotations about the primitive triclinic [1, 0, 0] axis.[27].

Eleven data sets were collected and the programs SADABS[28] or TWINABS[29] were applied for absorption correction. All structures were solved using direct methods as implemented in XS[30] and refined using XL.[30] All atoms were found after successive full-matrix least-squares refinement cycles on F^2 and refined with anisotropic thermal parameters. Hydrogen atoms were placed at calculated geometries and allowed to ride on the position of the parent atom. Hydrogen thermal parameters were set to 1.2 × the equivalent isotropic U of the parent atom.

Crystal structure data collected at 273, 290, and 293 K were refined in the *I*4/*m* space group where the molecule has required 4/*m* symmetry. The iron and nitrosyl nitrogen atoms are disordered over two positions equally occupied as required by the mirror plane that lies in the porphyrin plane. The nitrosyl oxygen atom is disordered over eight positions, four positions above and four positions below the porphyrin plane, equally occupied as required by the fourfold axis along the Fe–N_{NO} vector. The porphyrin phenyl groups are rotated 90° from the porphyrin plane with required mirror symmetry.

Crystal structure data collected at 33, 90, 100, 130, and 180 K were refined in $P\bar{1}$, Z = 1. However, alternatively they may be described in a nonstandard setting, $I\bar{1}$, Z = 2,[27] to more conveniently compare with the structures described in *I*4/*m*. The Fe–N–O unit is disordered over two positions equally occupied as required by the inversion symmetry. The four domains of the triclinic crystals are related by rotations about the [1, 0, 0] axis, which is coincident with the original Fe–N_{NO} bond.

Powder Diffraction Studies

Powder X-ray Diffraction (XRD) patterns were obtained on a Bruker Smart Apex I CCD diffractometer with graphite-monochromated Cu Kα (λ = 1.54178 Å) radiation from 100–300 K (700 Series Oxford Cryostream). Samples were mulled in Apiezon M vacuum grease, mounted on a glass fiber, and transferred to the cold gas stream of the diffractometer. Samples were equilibrated for 5 min at each temperature before data was collected. Data were collected with the 2D Apex detector fixed at 100 mm, 2θ = 12°, ϕ = 0°, and ω scanned between 0–20° over a 5 min. interval. Data were collected with both increasing and decreasing temperature. Data were integrated using the XRD[2] plug-in in the APEX II suite of programs[31] and further analyzed using the program EVA.[32].

DSC Measurements

The differential scanning calorimetry (DSC) measurements were performed at 150 to 400 K with 10 K/min heating rate using a Netzsch STA 404 DSC. Cooling was provided by liquid nitrogen boil-off. Temperature calibration was performed at the melting points of n-hexane, cyclohexane, octane, triply deionized water, gallium, naphthalene, indium, tin, and zinc. The scans were carried out in an atmosphere of flowing He (40 mL/min). A standard 40 μL aluminum crucible with a lid, which could be sealed hermetically with a crucible sealing press, was used for all experiments. Crucibles and lids were heated before experiments at about 570 K for 15 minutes to convert any hydroxides of aluminium that had been formed on the crucible surface to aluminum oxide. All DSC measurements were performed on 8–12 mg samples sealed under atmospheric conditions. Onset temperatures and enthalpies were deter-mined from 2 individual measurements using a software package supplied by the manufacturer. Reproducibility was confirmed using Setaram DSC 111.

Results

Crystal and molecular structures of [Fe(TPP)(NO)] have been obtained at 33, 90, 100, 130, 180, 273, 290, and 293 K on four different crystalline specimens. A reversible phase change from the tetragonal crystal system to the the triclinic crystal system was identified. Crystal

lographic details for all eleven structure determinations are summarized in Table 3. Thermal ellipsoid plots of [Fe(TPP)(NO)] at 33 K and 290 K are illustrated in Figure 1 and Figure 2. At 293 K [Fe(TPP)(NO)] has eight equally occupied NO orientations consistent with the previously reported structure at 298 K.[12] At 33 K [Fe(TPP)(NO)] has two equally occupied NO orientations consistent with the triclinic system. A number of diffraction experiments confirm the phase change that is also characterized by differential scanning calorimetry. Figure 3 gives representations of the I-centered cells at 33 and 293 K.

Discussion

Crystalline [Fe(TPP)(NO)] displays temperature-dependent phases that change from a tetragonal I-centered room-temperature phase to a triclinic phase at reduced temperatures. The triclinic phase can be described in terms of an I-centered triclinic cell that is a nonstandard crystallographic choice or as a standard primitive triclinic cell. The transition from room temperature to reduced temperature has been followed by differential scanning calorimetry. The DSC scan is illustrated in Figure 4. Two endotherms are observed that are centered at 280.4 K and 249.2 ± 0.2 K. The lower temperature transition is the one associated with the crystallo graphic phase change. The basis of the higher temperature transition is unclear; perhaps it is associated with a modest change in the porphyrin ring conformation. However, the structure determinations (at 273 and 293 K) that bracket this endotherm do not show any distinct, different features. We are thus unable to offer a conclusive explanation for this higher temperature transition.

We have also followed the phase change by examining the diffraction pattern over a range of temperatures. Figure S1 displays the predicted powder diffraction patterns at 100 and 290 K (Cu Kα radiation) that are based on the cell constants obtained from single crystals at those temperatures. The tetragonal reflection 101 (at 11.25° 2θ) cleanly splits into four resolved reflections on the decrease in crystal system symmetry. Accordingly, we focused on that region in a temperature-dependent powder diffraction measurement. Figure 5 displays the actual powder diffraction traces observed every 20° from 300 to 100 K. Figure S2 displays the change in intensity at the 11.25° 2θ position for both ascending and descending temperature and Figure 6 shows the intensity change for two triclinic reflections that are Laue equivalents in the tetragonal phase. Although the transition begins sharply at about 249 K, there does appear to be an asymmetry in the transition as the temperature is decreased which approaches the final complete change asymptotically. This behavior is also seen in two other regions where peaks in the two phases are sufficiently resolved to allow a measurement. These are the tetragonal reflection 231 (2θ = 25.57°) and 121 (2θ = 17.36°). These are also illustrated in Figure S2 of the SI. The calculation of the inflection point, also shown on the figure, are all at essentially the same temperature (243 to 248 K). A single-crystal data collection taken at 242 K, could not be indexed solely in terms of either the triclinic cell or the tetragonal cell but rather only in terms of both lattices. There may also be a slight asymmetry in the phase change between ascending and descending temperatures, but the complete reversibility is to be emphasized.

We have also measured the reflection profile of the (3 1 0) reflection on a point detector diffractometer (ω-scans). As the temperature is lowered, the peak begins to broaden between 252 and 248 K. The peak begins to split at 245 K and at 235 is well resolved into two peaks. Little further change occurs below 212 K. These ω-scan plots are given in Figure S3 of the SI. Single-crystal data collected at 180 K or lower are readily indexed in the triclinic cell and that at 273 K or higher in the tetragonal cell and the quality of the data sets appears to be similar in both crystal systems. Before describing the differences in the crystal structure between the two phases, we first describe the structure of [Fe(TPP)(NO)] in the two phases.

Molecular Structure of [Fe(TPP)(NO)] - *I*4/*m* Phase

The molecular structure of the room temperature phase of [Fe(TPP)(NO)] has been previously reported.[12] The complex's molecular structure agrees well with that previously reported. Complete details of all structure determinations in the tetragonal phase are given in the SI.

As displayed in Figure 1, the NO ligand is disordered over eight positions. The 4/*m* symmetry at the molecular center necessitates equal occupation of each of the eight positions. One common feature of iron(II) heme nitrosyls is the tilting of the Fe–N_{NO} vector.[13, 14] However, the nitrogen atom of NO is located on the 4-fold axis making any evaluation of ligand tilt impossible and the angle is nominally equal to 0°. Past experience suggests that if the off-axis tilts were similar to those observed previously,[14] the displacement of the NO nitrogen atom is just at the limit of leaving a trace in the thermal ellipsoid of the N atom. Any small changes in the position of nitrogen caused by the eight orientations make it very difficult to resolve a nitrogen position where the Fe–N vector is tilted off the heme normal. The uncertainties in the N–O bond length and FeNO bond angle are further accentuated by the uncertainty in the nitrogen position. The porphyrin ring is required to be precisely planar with the peripheral phenyl group making a dihedral angle of 90° with the central plane.

Molecular Structure of [Fe(TPP)(NO)] - *P*$\bar{1}$ Phase

The low-temperature phase of [Fe(TPP)(NO)] was refined in the *P*$\bar{1}$ setting. The fourfold symmetry observed in the tetragonal phase is reduced to inversion symmetry in the triclinic phase and hence, the NO oxygen is disordered only over two positions related by inversion symmetry. An ORTEP diagram of [Fe(TPP)(NO)] at 33 K is given in Figure 2. The ordering allows for a better description of the iron coordination parameters. The elimination of the NO rotational disordering reveals one hallmark feature of Fe(II) nitrosyl porphyrinates.[33] This feature is the off-axis tilting of the Fe–N_{NO} from the heme normal in the direction of the NO oxygen atom. At 33 K, the Fe–N_{NO} vector is tilted 6.3° off the heme normal in the direction of the NO oxygen atom. The Fe–N_{NO} off-axis tilts and several additional bonding parameters for [Fe(Por)(NO)] and related complexes are given in Table 2.[34–37] The tilt is also usually associated with an asymmetry in the equatorial Fe-N_p bonds. The two Fe–N_p bonds that bracket the NO ligand are shorter than the average whereas the other two are longer. This asymmetry is clearly a bonding effect. There is only a hint of this asymmetry for triclinic [Fe(TPP)(NO)]. At 33 K, the two short Fe–N_p bonds are 1.995(9) Å and 1.997(9) Å, whereas the long Fe–N_p bonds are 2.000(9) Å and 2.004(9) Å. The presence of the inversion center is likely to have led to obscuring of any in-plane asymmetry.

The porphyrin plane is required to be precisely planar in the tetragonal phase; in the triclinic phase there is no such requirement, but the core remains effectively planar with the largest core atom displacement from the best 24-atom plane only 0.03 Å (at 33 K). The out-of-plane displacement of iron is 0.20 Å, slightly less than seen in the tetragonal phase. The peripheral phenyl group, required to have exactly orthogonal dihedral angles in the tetragonal phase, have rotated slightly with dihedral angles between the phenyl plane and the core plane of 83.1 and 81.4°.

Phase Change

Why does the phase change occur? The phase change does not appear to lead to a substantial increase in the solid-state packing efficiency. The decrease in cell volume of ~3.5% between 90 and 293 K is similar to those seen in a number of other complexes over a similar temperature change and for which no phase change is observed.[38] Rather, the phase change appears to result from the fact that the [Fe(TPP)(NO)] molecule is intrinsically not as symmetric as it appears (and is required) in the tetragonal phase. This is partly, if not entirely, the consequence of the intrinsic off-axis tilt of the Fe–N_{NO} vector that has been observed in all well-ordered

(nitrosyl)iron porphyrinates. One explanation of the phase change is that it leads to an order–disorder transition that is sometimes observed on crystal cooling.[39] In this view, the intrinsically lower symmetry of the molecule is favored even though its solid-state structure does not pack with significantly larger efficiency. Nonetheless, the solid-state interaction of the porphyrin molecules display significant changes, as shown below.

An alternative idea is that the axial ligand distortion plays a fundamental role. As the temperature is decreased the Fe–NO off-axis tilt become increasingly favored. When the distortion occurs, the entire lattice will make small adjustments in the intermolecular packing that leads to the descent to triclinic symmetry and a single Fe–NO orientation above the porphyrin plane. That the NO tilting is driving the phase change is consistent with the observation of four crystal domains, with relative rotations of either 90 or 180° with respect to the major domain. The rotations are along the original Fe–NO axis, consistent with the four possible tilt direction choices. Of course a similar change must occur on the other side of the porphyrin plane since that side of the porphyrin plane is also populated in the tetragonal phase. The reasons for the preservation of an inversion center at the porphyrin ring center is that it is the most symmetric of the possible orientations of the FeNO group and leads to the preservation of the intrinsic NO-induced asymmetry of the Fe interaction with the porphyrin nitrogen atoms (core asymmetry).

The phase change leads to asymmetry in the environment of an individual [Fe(TPP)(NO)] molecule. The I-centered triclinic cell constants are a = 13.373(3), b = 13.353(4), c = 9.745(2) Å, α = 99.310(17), β = 93.651(15), and γ = 90.64(2)° and are clearly similar to those of the tetragonal phase. This has been shown in Figure 3. In the triclinic system the porphyrin planes are in the *xy* plane, and form parallel layers of porphyrin molecules comparable to the planes parallel to the *xy* plane in the tetragonal phase. However, in the tetragonal phase the porphyrin layers are exactly superimposed, but in the triclinic phase the molecules are no longer directly above each other as a result of the 9.3° tilt of the porphyrin planes from the *c* axis. Distances between molecular centers reflect this change. The fourteen closest intermolecular center···center distances in both crystal systems are given in Table 3. The closest pair of contacts to the target molecule remain the pair related by a translation perpendicular to the molecular array direction. The next eight closest contacts are all equal in the tetragonal system. In the triclinic system, the analogously related intermolecular distances are either shorter or longer and fall along the the body diagonals in pairs and are summarized in Table 3. One of the consequences of the resulting asymmetry is that the intermolecular contacts now constrain the FeNO group to a single allowed orientation on each side of the porphyrin plane in the triclinic phase. This also allows the observation of the off-axis tilt of the Fe–NO vector in the triclinic phase that, if present in the tetragonal system, will be obscured by the crystallographically required symmetry.

Summary

Crystalline [Fe(TPP)(NO)] is found to undergo a reversible temperature-dependent phase change from tetragonal to triclinic. In the lower symmetry crystal system, the intrinsic off-axis tilt of the Fe–NO vector from the porphyrin plane becomes apparent. Two suggestions for the origin of the phase change are given.

Supplementary Material

Refer to Web version on PubMed Central for supplementary material.

Acknowledgments

We thank the National Institutes of Health for support of this research under Grant GM-38401 (W.R.S) and the NSF for X-ray instrumentation support through Grant CHE-0443233. M.M.O. thanks the the University of California., Davis for the He diffraction setup. We acknowledge Olga Trofymluk, Department of Chemistry, Thermochemistry Facility, University of California, Davis for providing assistance with the DSC results. The thoughtful remarks of the reviewers helped significantly in the final form of this paper.

References and Notes

1. Culotta E, Koshland DE. Science 1992;258:1862. [PubMed: 1361684]
2. Rapoport RM, Murad F. Circ. Res 1983;52:352. [PubMed: 6297832]
3. Ignarro LJ, Adams JB, Horwitz PM, Wood KS. J. Biol. Chem 1986;261:4997. [PubMed: 2870064]
4. Azuma H, Ishikawa M, Sekizaki S. Br. J. Pharmacol 1986;88:411. [PubMed: 3089351]Furlong B, Henderson AH, Lewis MJ, Smith JA. Br. J. Pharmacol 1987;90:687. [PubMed: 3495310]Radomski MW, Palmer RMJ, Moncada S. Br. J. Pharmacol 1987;92:639. [PubMed: 3322462]
5. Garthwaite J. Trends Neurosci 1991;14:60. [PubMed: 1708538]
6. Koshland DE Jr. Science 1992;258:1861. [PubMed: 1470903]Butler AR, Williams DLH. Chem. Soc. Rev 1993:233.Moncada S, Palmer RMJ, Higgs EA. Pharmacol. Rev 1991;43:109. [PubMed: 1852778]
7. Marletta MA. J. Biol. Chem 1993;17:12231. [PubMed: 7685338]
8. Griffith OW, Stuehr DJ. Annu. Rev. Physiol 1995;57:707. [PubMed: 7539994]
9. Alderton WK, Cooper CE, Knowles RG. Biochem. J 2001;357:593. [PubMed: 11463332]Griffith OW, Stuehr DJ. Annu. Rev. Physiol 1995;57:707. [PubMed: 7539994]
10. Averill BA. Chem. Rev 1996;96:2951. [PubMed: 11848847]Eich RF, Li T, Lemon DD, Doherty DH, Curry SR, Aitken JF, Mathews AJ, Johnson KA, Smith RD, Phillips GN Jr. Olson JS. Biochemistry 1996;35:6976. [PubMed: 8679521]
11. The following abbreviation ts used in this paper. OEP, dianion of octaethylporphyrin; oxoOEC dianion of oxooctaethylchlorin, (3,3,7,8,12,13,17,18-octaethyl-(3H)-porphin-2-onato(2-); OETAP, dianion of octaethyltetraphenylporphyrin; TPP, dianion of *meso*-tetraphenylporphyrin; $TPPBr_4$, dianion of 2,3,12,13-tetrabromortetraahenylporhyrin; N_p, porphinato nitrogen atom.
12. Scheidt WR, Frisse ME. J. Am. Chem. Soc 1975;97:17. [PubMed: 1133330]
13. Ellison MK, Scheidt WR. J. Am. Chem. Soc 1997;119:7404.
14. Scheidt WR, Duval HF, Neal TJ, Ellison MK. J. Am. Chem. Soc 2000;122:4651.
15. Leu BM, Zgierski MZ, Wyllie GRA, Scheidt WR, Sturhahn W, Alp EE, Durbin SM, Sage JT. J. Am. Chem. Soc 2004;126:4211. [PubMed: 15053610]
16. Praneeth VKK, Näther C, Peters G, Lehnert N. Inorg. Chem 2006;45:2795. [PubMed: 16562937]
17. Ghosh A, Wondimagegn T. J. Am. Chem. Soc 2000;122:8101.Ghosh A. Acc. Chem. Res 2005;38:943. [PubMed: 16359166]
18. Cheng L, Novozhilova I, Kim C, Kovalevsky A, Bagley KA, Coppens P, Richter-Addo GB. J. Am. Chem. Soc 2000;122:7142.
19. Scheidt WR, Durbin SM, Sage JT. J. Inorg. Biochem 2005;99:60. [PubMed: 15598492]
20. Silvernail NJ, Sage JT, Alp EE, Sturhahn W, Zhang Z, Scheidt WR. There does not appear to be a relationship in these phenomena. work in progress.
21. Dodd, RE.; Robinson, PL. Experimental Inorganic Chemistry. New York: Elsevier; 1957. p. 253
22. Adler AD, Longo FR, Finarelli JD, Goldmacher J, Assour J, Korsakoff L. J. Org. Chem 1967;32:476.
23. Adler AD, Longo FR, Kampus F, Kim J. J. Inorg. Nucl. Chem 1970;32:2443.
24. The Oxford control unit is calibrated at the factory using the phase change of Rochelle's salt at 109 K.25 The factory calibration was checked in our laboratory with a well-insulated iron-constantan thermocouple and an Omega 199 temperature meter. All reported temperatures are believed accurate to within 2 K.
25. Tomaszewski PE. Phase Trans 1992;38:127.
26. Sheldrick, GM. cell_now. Madison, WI: Bruker-Nonius AXS; 2001.

27. The transformation matrix (**M**) converts *P*↿, Z = 1 to *I*↿, Z = 2. M=|01−1−111100| The rotations in the triclinic I-centered cell are about the *c*-axis.
28. Sheldrick, GM. SADABS. Göttingen, Germany: Universität Göttingen; 2006.
29. Sheldrick, GM. TWINABS. Göttingen, Germany: Universität Göttingen; 2006.
30. Sheldrick GM. Acta Cryst 2008;A64:112.
31. APEX-II. Madison, WI: Bruker-Nonius AXS; 2004.
32. EVA. Madison, WI: Bruker-Nonius AXS; 2002.
33. Wyllie GRA, Scheidt WR. Chem. Rev 2002;102:1067. [PubMed: 11942787]
34. Bohle DS, Debrunner P, Fitzgerald J, Hansert B, Hung C-H, Thompson AJ. J. Chem. Soc., Chem. Commun 1997:91.
35. Ellison MK, Schulz CE, Scheidt WR. Inorg. Chem 2000;39:5102. [PubMed: 11233208]
36. Scheidt WR, Lee YJ, Hatano K. J. Am. Chem. Soc 1984;106:3191.
37. Silvernail NJ, Noll BC, Scheidt WR. Inorg. Chem 2006;45:7050. [PubMed: 16933901]
38. Silvernail NJ, Pavlik JW, Noll BC, Schulz CE, Scheidt WR. Inorg. Chem 2008;47:912. [PubMed: 18173262]
39. Kubicki M. Acta Crystallogr., Sect. B 2004;B60:333. [PubMed: 15148437]and references therein.

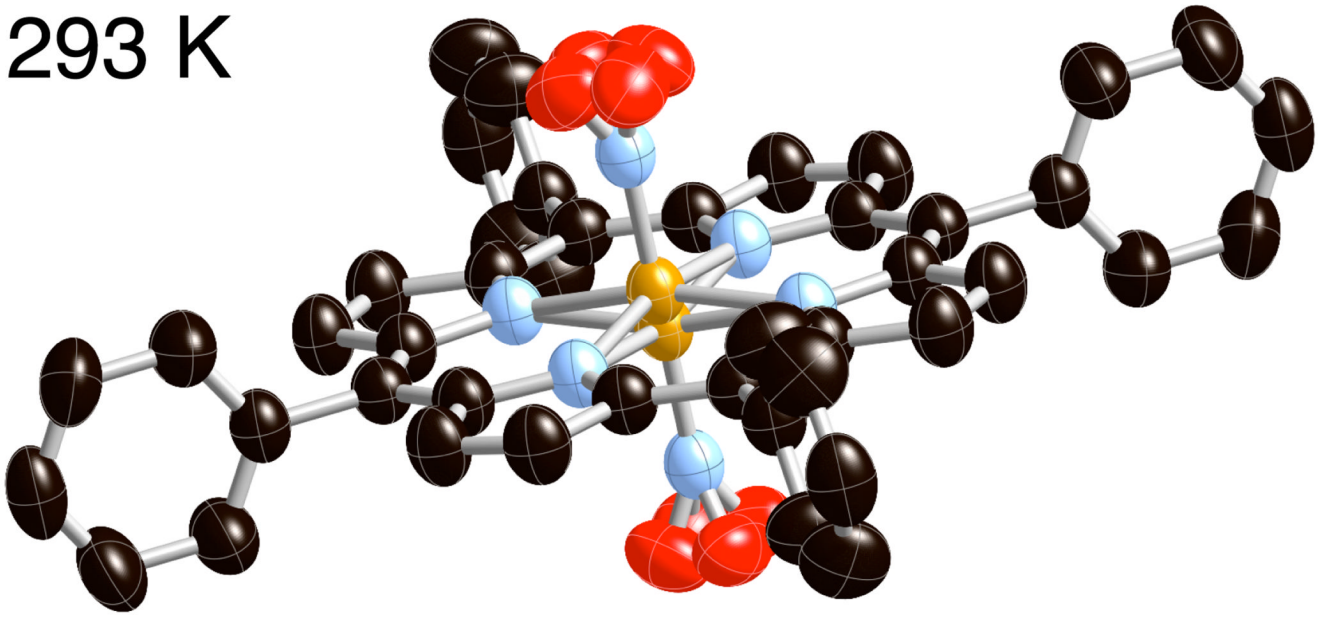

Figure 1.
Thermal ellipsoid plot of [Fe(TPP)(NO)] at 293 K (50% probability ellipsoids). Hydrogen atoms are omitted for clarity.

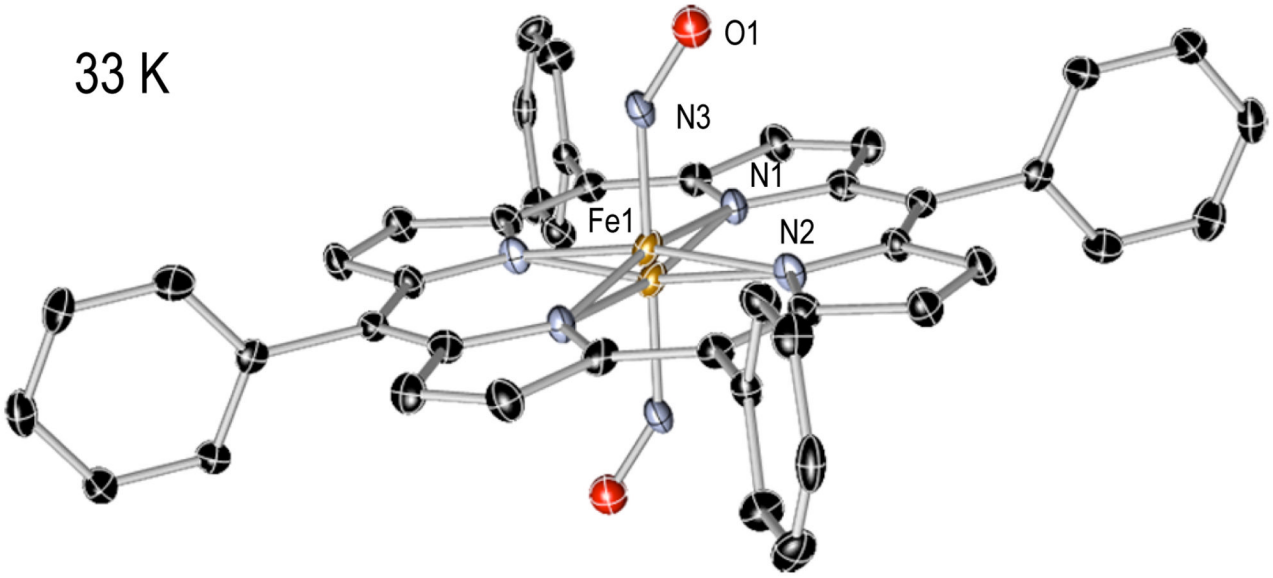

Figure 2.
Thermal ellipsoid plot of [Fe(TPP)(NO)] at 33 K (50% probability ellipsoids). Hydrogen atoms are omitted for clarity.

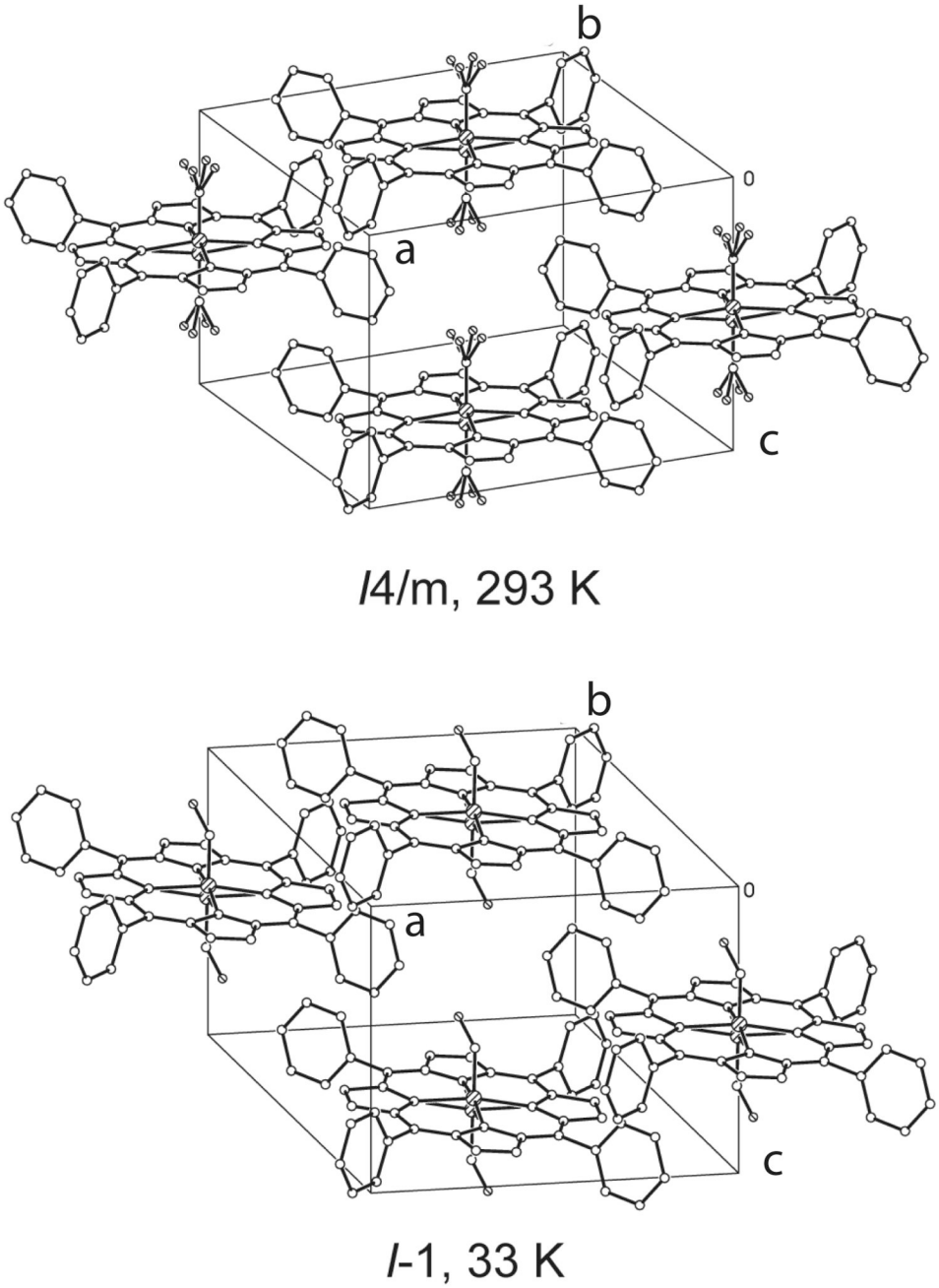

Figure 3.

Diagrams of the tetragonal and triclinic I-centered cells showing the effects of the partial order-disorder phase transition. At 33 K the Fe–NO group retains the disorder with respect to crystallographic inversion but the disorder of the NO group due to fourfold symmetry has been removed. In the tetragonal phase the porphyrin plane is perpendicular to the *c* axis, but is tipped by 9.3° from the perpendicular to the *c* axis in the triclinic phase.

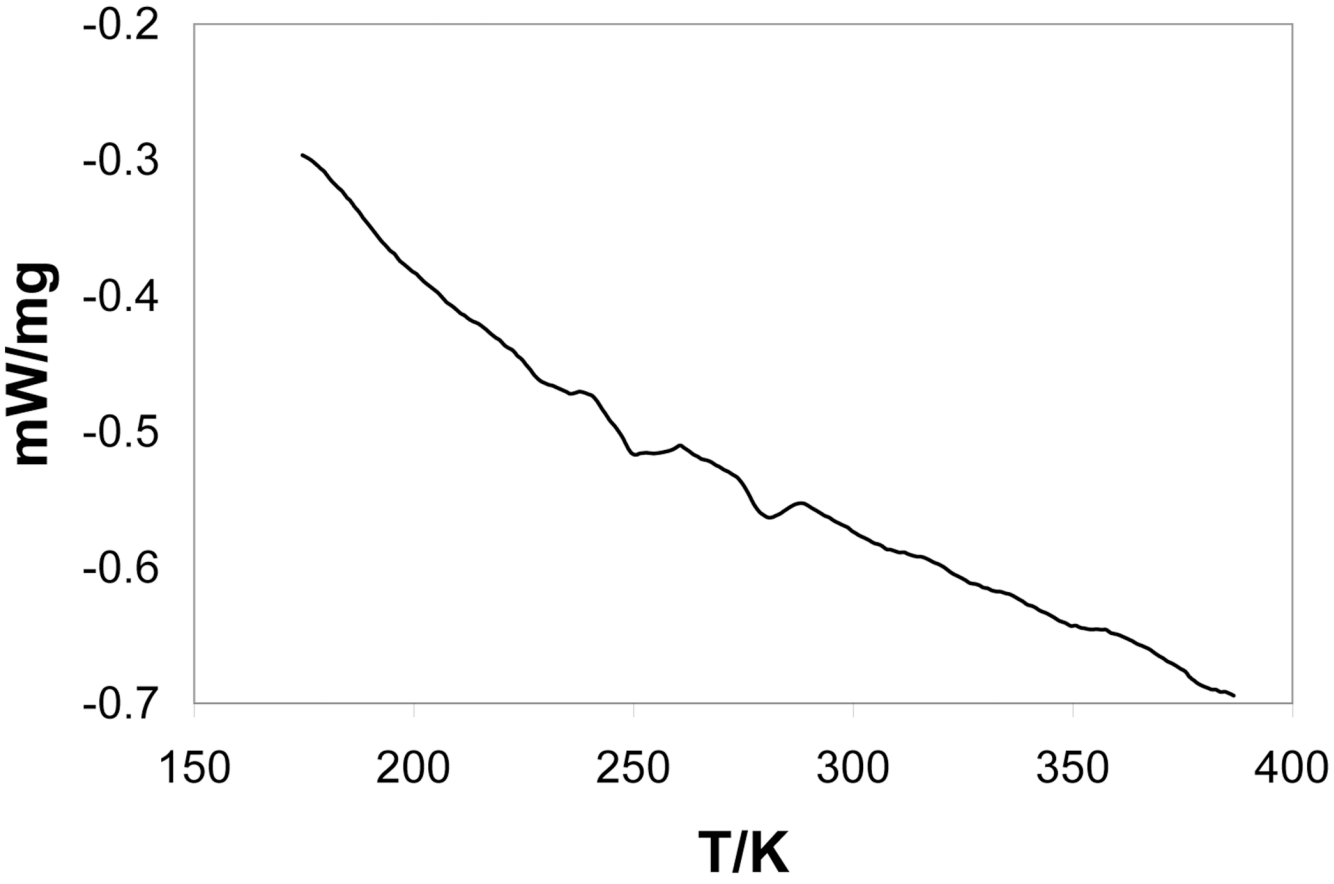

Figure 4.
DSC scan for [Fe(TPP)(NO)]. The endotherms are centered at 280.4 and 249.2 ± 0.2 K. The lower temperature transition corresponds to the observed crystallographic phase change.

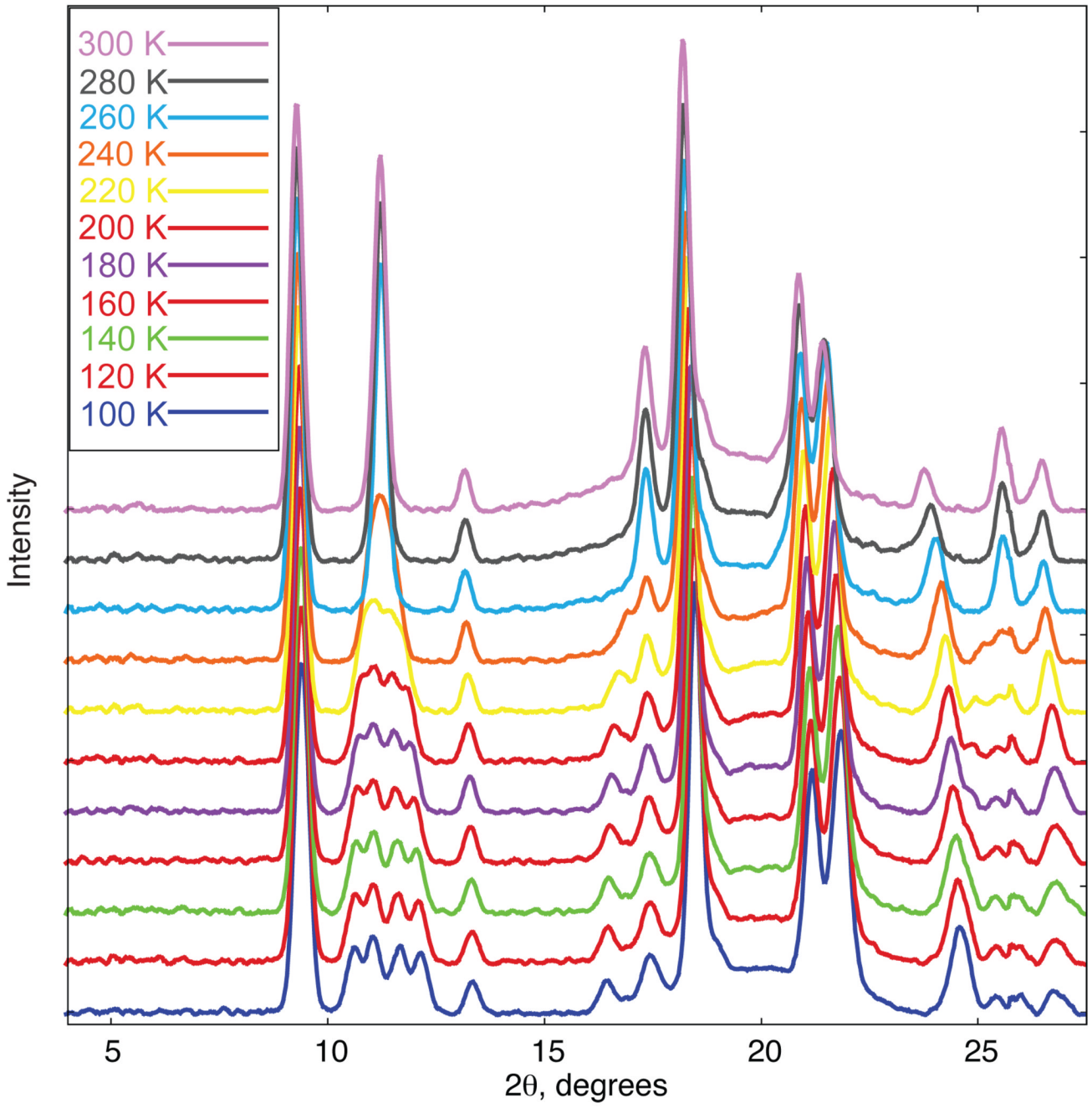

Figure 5.
X-ray powder diffraction spectra of [Fe(TPP)NO)] from 100 to 300 K at 20 degree increments.

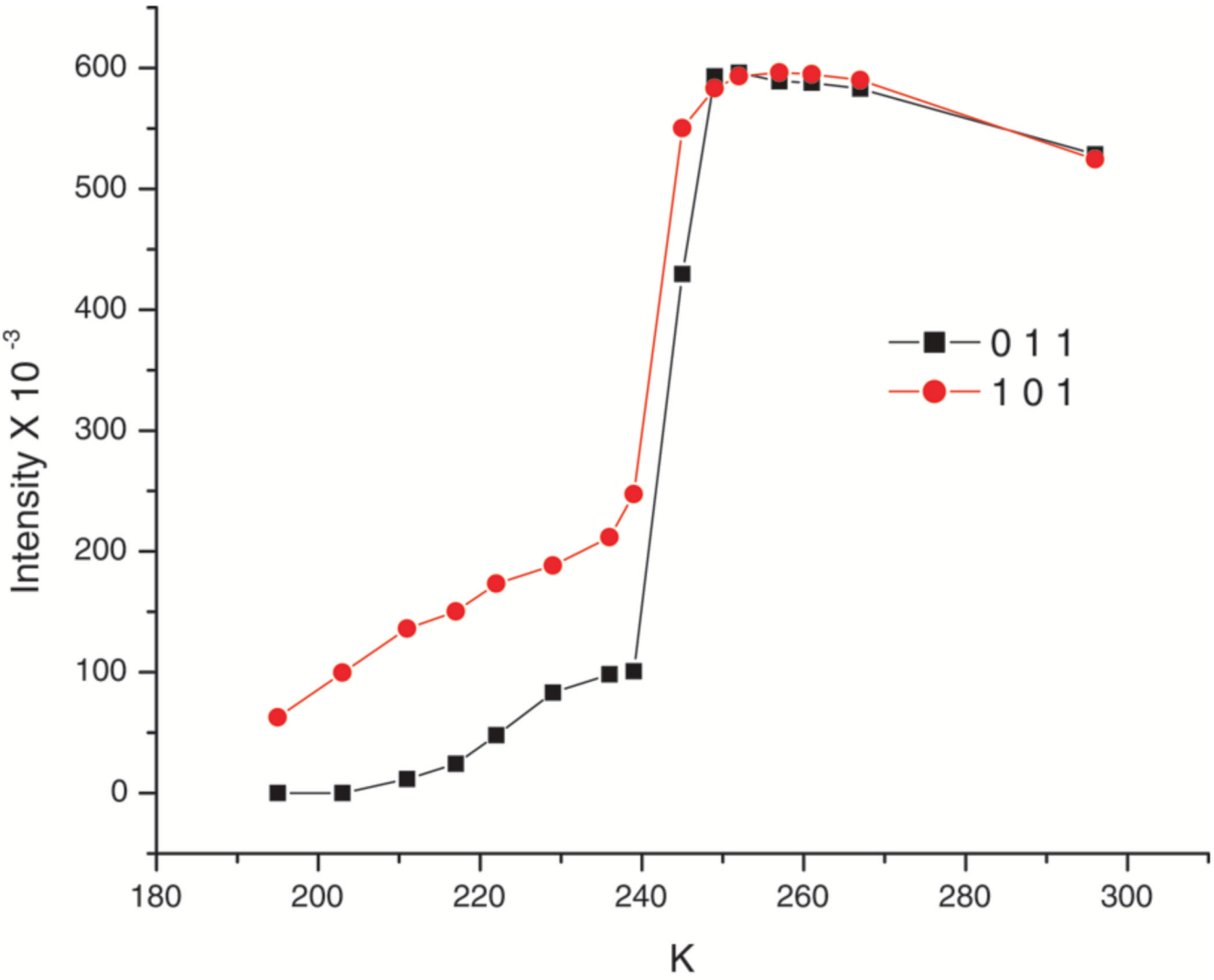

Figure 6.
A plot of measured intensities on a single crystal of Fe(TPP)(NO). Above the transition point the reflections (0 1 1) and (1 0 1) are Laue equivalents in the tetragonal cell and the quality of the data sets for the two phases appear similar. They become inequivalent at the phase change near 24 °C. The decrease in the intensities at the higher temperature can be ascribed to the effects of thermal motion.

Table 1

Summary of Crystallographic Data for [Fe(TPP)(NO)] at several temperatures.

temp, K, cryst. #	*a*, Å	*b*, Å	*c*, Å	α, deg	β, deg	γ, deg	*V*/*Z*, Å^3	unique data	obs. data[a]	final *R*	final wR_2
33, 1[b]	9.745(2)	9.867(2)	10.375(3)	82.66(2)	66.01(2)	70.05(2)	856.7(4)	4221	2476	0.0486	0.0884
90, 1[b]	9.754(2)	9.943(2)	10.394(3)	82.25(2)	65.78(2)	69.44(2)	855.81(4)	4337	2843	0.0476	0.1084
100, 2[b]	9.7310(8)	9.9238(8)	10.3902(6)	82.195(1)	65.693(4)	69.384(5)	855.8(1)	6497	4766	0.0449	0.1213
100, 3[b]	9.734(3)	9.960(3)	10.391(3)	82.100(3)	65.63(2)	69.25(2)	858.0(4)	5092	4085	0.0788	0.1979
100, 4[b]	9.7201(7)	9.9105(6)	10.3715(6)	82.304(4)	65.802(4)	69.546(4)	853.81(9)	6741	4480	0.0638	0.1543
130, 4[b]	9.7394(10)	9.9634(10)	10.3998(10)	82.078(4)	65.661(4)	69.225(4)	859.65(15)	4103	3204	0.0537	0.1354
180, 1[b]	9.765(2)	10.120(2)	10.466(2)	81.35(2)	65.23(2)	68.12(2)	871.4(4)	4628	2579	0.0481	0.0981
273, 4[c]	13.4152(2)	13.4152(2)	9.7151(3)	90	90	90	874.2(7)	1101	918	0.0391	0.1132
290, 2[c]	13.4466(3)	13.4466(3)	9.7498(5)	90	90	90	881.43(5)	1155	973	0.0340	0.0996
293, 1[c]	13.4748(12)	13.4748(12)	9.7686(18)	90	90	90	886.9(2)	1081	842	0.0351	0.0989
293, 2[c]	13.4502(3)	13.4502(3)	9.7533(4)	90	90	90	882.23(5)	1108	881	0.0372	0.1024
293,0[c,d]	13.468(4)	13.468(4)	9.755(8)	90	90	90			951	0.044	

[a] $[I > 2\sigma(I)]$.

[b] triclinic, $P\bar{1}$.

[c] tetragonal, $I4/m$.

[d] see ref. 12.

Inorg Chem. Author manuscript; available in PMC 2010 February 2.

Table 2

Notable Bonding Parameters for [Fe(TPP)(NO)] and related compounds.

Complex, temp., and crystal	Fe–XY[a]	X–Y[a]	Fe–X–Y[b]	<Fe–$N_{p¿}$[a]	ΔFe[d]	Fe–N, tilt[b]	νX–Y[c]	ref
[Fe(TPP)(NO)], 33 K, 1	1.739(6)	1.163(5)	144.4(5)	1.999(4)	0.20	6.3		tw
[Fe(TPP)(NO)], 90 K, 1	1.740(5)	1.153(4)	145.6(4)	1.997(13)	0.20	5.8		tw
[Fe(TPP)(NO)], 180 K, 1	1.737(5)	1.131(4)	147.3(4)	2.002(14)	0.21	4.7		tw
[Fe(TPP)(NO)], 293 K, 1	1.720(6)	1.107(11)	149.5(7)	2.0005	0.23	[e]	1670/1700[f]	tw
[Fe(TPP)(NO)]	1.722(2)	1.167(3)	144.4(2)	2.004(15)	0.29	[e]	1670[f]	12
[Fe(TPPBr_4)(NO)](**A′**)	1.734(8)	1.119(11)	147.9(8)	2.01(3)	0.37	5.6	1678[g]	14
[Fe(TPPBr_4)(NO)](**A″**)	1.726(9)	1.144(12)	146.9(9)	2.00(2)	0.32	7.1	1678[g]	14
[Fe(TPPBr_4)(NO)](**B**)	1.691(11)	1.145(16)	145(1)	1.95(3)	0.29		1681[g]	14
[Fe(OEP)(NO)](**A**)	1.722(2)	1.167(3)	144.4(2)	2.004(15)	0.29	6.5	1666[g]	13,14
[Fe(OEP)(NO)](**B**)	1.7307(7)	1.1677(11)	142.74(8)	2.009(12)	0.27	8.2	1673[g]	13,14
[Fe(oxoOEC)(NO)]	1.7320(13)	1.1696(19)	143.11(15)	2.009(9)	0.26	7.1	1690[g]	14
[Fe(OETAP)(NO)]	1.721(4)	1.155(5)	143.7(4)	1.932(9)	0.31	7.6	1666[g]	34
$[Fe(OEP)(NO)]^+$	1.6528(13)	1.140(2)	173.19(13)	1.994(5)	0.32	4.6	1838[g]	35
$[Fe(OEP)(NO)]^+$	1.644(3)	1.112(4)	176.9(3)	1.994(1)	0.29	0.6	1868[g]	36
[Fe(OEP)(CO)]	1.7140(11)	1.1463(12)	177.20(8)	1.988(2)	0.20	3.8	1944[g]	37
[Fe(OEP)(CO)]·C_6H_6	1.7077(13)	1.1259(16)	177.20(11)	1.984(3)	0.22	2.4	1948[g]	37
[Fe(OEP)$(CO)_2$]	1.8558(10)	1.1216(13)	173.95(9)	2.0133(7)	0.00	5.9	2021[g]	37

[a] Å

[b] degrees.

[c] cm^{-1}.

[d] Displacement from 24-atom mean plane.

[e] Value not determined, obscured by crystallographic symmetry.

[f] KBr pellet.

[g] Nujol mull.

Table 3

Molecule center to center distances and symmetry operators for [Fe(TPP)(NO)] in the $I\bar{1}$ (33 K) and $I4/m$ (293 K) phases from crystal 1.

symmetry position	x, y, z	$I\bar{1}$ Ct···Ct Å	$I4/m$ Ct···Ct Å	Difference Å
x, *y*, *z*	1/2, 1/2, 0	0	0	0
x, *y*, *z* + 1	1/2, 1/2, 1	9.745	9.769	−0.024
x, *y*, *z* − 1	1/2, 1/2, −1	9.745	9.769	−0.024
−*x*, −*y*, −*z*	1, 1, 1/2	9.867	10.707	−0.840
−*x* − 1, −*y* − 1, −*z* − 1	0, 0, −1/2	9.867	10.707	−0.840
−*x*, −*y* −1, −*z*	1, 0, 1/2	10.973	10.707	0.266
−*x* − 1, −*y*, −*z* − 1	0, 1, −1/2	10.973	10.707	0.266
−*x* − 1, −*y*, −*z*	0, 1, 1/2	10.375	10.707	−0.332
−*x*, −*y* −1,−*z* − 1	1, 0, −1/2	10.375	10.707	−0.332
−*x* − 1, −*y* − 1, −*z*	0, 0, 1/2	11.256	10.707	0.549
−*x*, −*y*, −*z* − 1	1, 1, −1/2	11.256	10.707	0.549
x + 1, *y*, *z*	3/2, 1/2, 0	13.373	13.475	−0.102
x − 1, *y*, *z*	−1/2, 1/2, 0	13.373	13.475	−0.102
x, *y* + 1, *z*	1/2, 3/2, 0	13.353	13.475	−0.122
x, *y* − 1, *z*	1/2, −1/2, 0	13.353	13.475	−0.122

[a] (Ct···Ct in $I\bar{1}$) − (Ct···Ct in $I4/m$).